

# Prolonged magmatic activity on Mars inferred from the detection of felsic rocks

James J. Wray<sup>1\*</sup>, Sarah T. Hansen<sup>1</sup>, Josef Dufek<sup>1</sup>, Gregg A. Swayze<sup>2</sup>, Scott L. Murchie<sup>3</sup>, Frank P. Seelos<sup>3</sup>, John R. Skok<sup>4</sup>, Rossman P. Irwin III<sup>5</sup> and Mark S. Ghiorso<sup>6</sup>

**Rocks dominated by the silicate minerals quartz and feldspar are abundant in Earth's upper continental crust<sup>1</sup>. Yet felsic rocks have not been widely identified on Mars<sup>2</sup>, a planet that seems to lack plate tectonics and the associated magmatic processes that can produce evolved siliceous melts on Earth<sup>3</sup>. If Mars once had a feldspar-rich crust that crystallized from an early magma ocean such as that on the Moon, erosion, sedimentation and volcanism have erased any clear surface evidence for widespread felsic materials. Here we report near-infrared spectral evidence from the Compact Reconnaissance Imaging Spectrometer for Mars onboard the Mars Reconnaissance Orbiter for felsic rocks in three geographically disparate locations on Mars. Spectral characteristics resemble those of feldspar-rich lunar anorthosites<sup>4,5</sup>, but are accompanied by secondary alteration products (clay minerals). Thermodynamic phase equilibrium calculations demonstrate that fractional crystallization of magma compositionally similar to volcanic flows near one of the detection sites can yield residual melts with compositions consistent with our observations. In addition to an origin by significant magma evolution, the presence of felsic materials could also be explained by feldspar enrichment by fluvial weathering processes. Our finding of felsic materials in several locations on Mars suggests that similar observations by the Curiosity rover in Gale crater<sup>6</sup> may be more widely applicable across the planet.**

Felsic rocks, such as granite and its volcanic equivalent, rhyolite, form commonly on Earth in subduction zones through partial melting or fractional crystallization in the shallow crust; in bimodal basalt–rhyolite suites associated with hotspot volcanism; or in some rocks formed during the Archaean era, when a steeper geothermal gradient facilitated intraplate partial melting of basalts at relatively shallow depths<sup>1</sup>. Anorthosite, a rock with >90% feldspars, can form in low-density cumulate layers in a slowly cooling mafic magma chamber, occasionally coalescing into plutons in Proterozoic cratonic settings<sup>1</sup>. Anorthosite is hypothesized to have formed globally on Earth's Moon through similar processes in a primordial magma ocean<sup>7</sup>.

Mars retains no incontrovertible evidence of plate tectonics<sup>3</sup> and any magma ocean that it once had must have formed very early and subsequently been buried or modified beyond recognition. It is also possible that felsic rocks never formed on Mars in proportions comparable to the Moon<sup>7</sup>. The exposed crust of Mars has been interpreted as primarily basaltic<sup>2,8,9</sup>. Although some regions are spectrally consistent with andesite<sup>9</sup>, these have alternatively been interpreted as weathered basalt<sup>10,11</sup> or glass<sup>12</sup>. Mars Pathfinder

identified rocks with the chemical composition of basalt–andesite to andesite<sup>13</sup>, but these too can be attributed to weathering rinds<sup>2</sup>. Localized quartz detected on Mars was initially attributed to evolved magmas<sup>14</sup> but can instead be explained as a secondary phase formed hydrothermally or through diagenetic maturation of opaline silica detected in the same locations<sup>15,16</sup>. The only widely accepted example of intermediate-to-felsic igneous rocks on Mars is a unit in the Nili Patera caldera of Syrtis Major, identified as dacitic based on thermal infrared spectroscopy<sup>17</sup>.

Here, we describe one large region and two smaller locations where felsic materials have been identified using the Compact Reconnaissance Imaging Spectrometer for Mars (CRISM) aboard the Mars Reconnaissance Orbiter. Such feldspar-rich rocks were not anticipated on Mars, therefore none of CRISM's standard parameters for mineral mapping (see Supplementary Information) are designed to identify them. A global search for felsic materials is further challenged by several mechanisms whereby common mineral mixtures can produce false detections<sup>18</sup>. After identifying felsic materials in Xanthe Terra, we focused our analyses on Syrtis Major, the only large martian volcano whose bedrock compositions and textures are not obscured by mantling dust<sup>8</sup>, and northeast Noachis Terra in the southern highlands, which has the densest concentration of exposed intercrater and crater-floor bedrock on Mars<sup>19,20</sup>.

Felsic materials are difficult to identify through near-infrared spectroscopy. Pure quartz and feldspar are nominally undetectable in CRISM's 0.4–3.9  $\mu\text{m}$  wavelength range, but some feldspars exhibit a broad absorption centred at  $\sim 1.25$ – $1.31$   $\mu\text{m}$  (ref. 21) owing to minor substitution of  $\text{Fe}^{2+}$  for  $\text{Ca}^{2+}$  (ref. 22). This absorption is typically much weaker than the  $\sim 1$   $\mu\text{m}$  absorption of Fe-rich phases such as olivine and pyroxene and is generally detectable only in very feldspar-rich rocks with <5% associated mafics (as found in some areas on the Moon<sup>4,5</sup>).

A  $\sim 1.3$   $\mu\text{m}$  absorption band is the strongest spectral feature observed in the 0.7–2.6  $\mu\text{m}$  wavelength range at each location discussed here (Fig. 1). We attribute this feature to  $\text{Fe}^{2+}$  in feldspar. The feature is visible in CRISM reflectance spectra (Fig. 1a) and accentuated when the spectra are ratioed to nearby spectrally neutral areas (Fig. 1b). The only other minerals in our spectral libraries with a similarly broad absorption centred at 1.23–1.32  $\mu\text{m}$  are  $\text{Fe}^{2+}$ -bearing garnets, such as almandine (Fig. 1c). However, such garnets have a comparably broad (and half as deep) absorption at  $\sim 1.7$   $\mu\text{m}$ , not observed in any of our CRISM spectra. Our CRISM ratio spectra show no absorptions near 1  $\mu\text{m}$ , suggesting pyroxene and olivine abundances <5% (refs 4,5). The presence of feldspars

<sup>1</sup>School of Earth and Atmospheric Sciences, Georgia Institute of Technology, Atlanta, Georgia 30332, USA, <sup>2</sup>US Geological Survey, Denver, Colorado 80225, USA, <sup>3</sup>Applied Physics Laboratory, Johns Hopkins University, Laurel, Maryland 20723, USA, <sup>4</sup>Department of Geology and Geophysics, Louisiana State University, Baton Rouge, Louisiana 70803, USA, <sup>5</sup>Center for Earth and Planetary Studies, National Air and Space Museum, Smithsonian Institution, Washington DC 20013, USA, <sup>6</sup>OFM Research, Seattle, Washington 98115, USA. \*e-mail: [jwray@gatech.edu](mailto:jwray@gatech.edu)

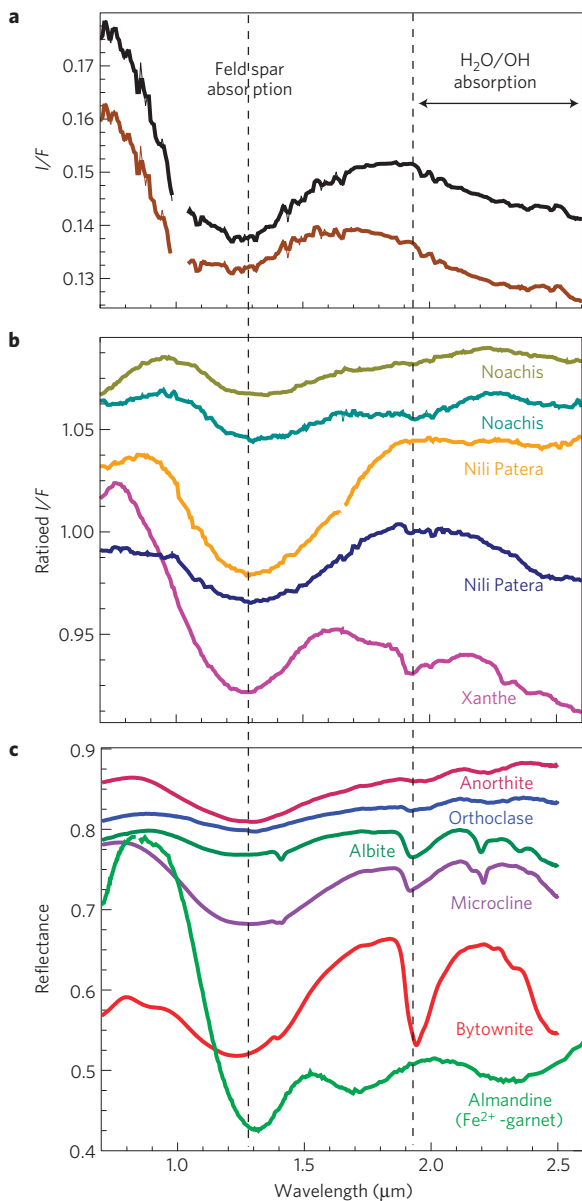


**Figure 1 | Martian and laboratory spectra of feldspar-rich materials.**

**a**, CRISM  $I/F$  spectra from FRT000082EE in Nili Patera.  $I/F$  is the ratio of measured radiance to incoming solar flux. Feldspar-rich areas (black) are brighter and have a broad minimum at  $\sim 1.25\text{--}1.3\ \mu\text{m}$  not observed elsewhere in the scene (brown). **b**, CRISM spectral ratios, vertically offset for clarity, from FRT00008F08 in Noachis Terra, FRT000082EE in Nili Patera and HRL0000927F in Xanthe Terra. Narrow absorptions at 1.9, 2.2, 2.3 or  $2.4\ \mu\text{m}$  and negative slopes across this range in some CRISM and library spectra are attributable to minor  $\text{H}_2\text{O/OH}$ -bearing phases. **c**, US Geological Survey library spectra of feldspars and garnet.

and the very low abundance of mafic minerals strongly indicate a felsic composition. Many of the CRISM and library spectra have weaker absorptions at 1.9 and  $2.2\text{--}2.5\ \mu\text{m}$  from  $\text{H}_2\text{O}$  and OH in accessory phases or alteration products. Anhydrous quartz has no diagnostic features in the spectral range of CRISM, so we cannot constrain its abundance.

The  $1.3\ \mu\text{m}$  absorption band increases in depth and wavelength with increasing FeO content in the feldspar<sup>22</sup> and is also affected by particle size and crystallinity. Early lab studies suggested spectral trends with composition within the plagioclase series<sup>21</sup>, but the band depth and position display no clear

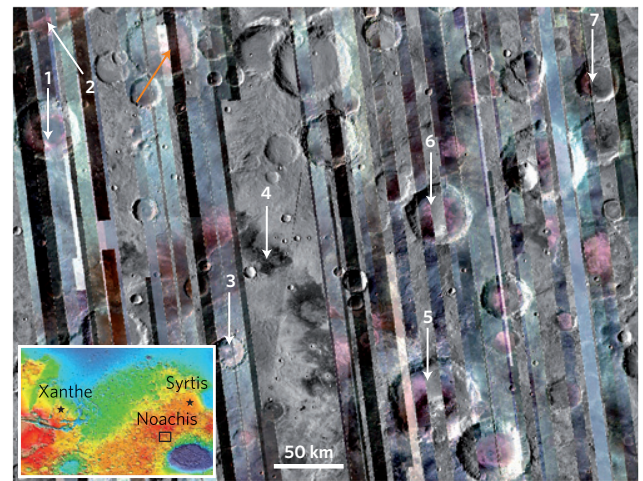


**Figure 2 | Felsic materials in Noachis Terra.** CRISM multispectral reflectances (red,  $2.53\ \mu\text{m}$ ; green,  $1.33\ \mu\text{m}$ ; blue,  $0.77\ \mu\text{m}$ ) overlain on the THEMIS daytime infrared mosaic (greyscale, with high thermal inertia materials including the felsic rocks appearing dark). The bright pink materials on many large crater floors are felsic. The orange arrow points to the source area for the gold and teal spectra in Fig. 1b and white arrows indicate other locations where felsic rocks have been identified using higher resolution CRISM hyperspectral data. The image is centred at  $22.8^\circ\ \text{S}$ ,  $44.6^\circ\ \text{E}$ ; inset shows its location (black box) on Mars Orbiter Laser Altimeter topography spanning  $60^\circ\ \text{S}$  to  $60^\circ\ \text{N}$ ,  $90^\circ\ \text{W}$  to  $90^\circ\ \text{E}$ . Numbers are referred to in the main text.

trends with feldspar composition among our library spectra (Fig. 1c). Near-infrared analysis is therefore insufficient to uniquely determine feldspar and rock types, but geologic context provides additional constraints.

Felsic materials were first identified in CRISM data in the wall of a small valley in Xanthe Terra north of Valles Marineris (Supplementary Fig. 1); the valley terminates in Camichel crater,  $\sim 65\ \text{km}$  in diameter ( $D$ ). At the valley mouth is a large fan-shaped deposit with strong spectral signatures of hydrous silica in its distal lobe<sup>23</sup>. The felsic materials are exposed in a  $\sim 1\text{-km}$ -wide light-toned debris apron shedding from the upper valley wall (Supplementary Fig. 1b) and their spectral absorptions at 1.9, 2.3 and  $2.4\ \mu\text{m}$  (Fig. 1b, magenta) are attributable to Fe/Mg-smectite clays associated with the feldspars. Kaolinite is present in a separate valley wall outcrop  $\sim 1\ \text{km}$  upstream. The limited exposure of this buried felsic material precludes direct study of its morphology and distribution.

Broader felsic outcrops spanning tens of square kilometres each occur on large crater floors and intercrater plains of northeast Noachis Terra (Fig. 2). In one  $D \sim 52\ \text{km}$  crater (Fig. 2, orange arrow), aqueous activity before and after emplacement of the felsic unit is evidenced by Al- and Fe/Mg-smectites in the pre-existing crater wall rocks and sinuous ridges (interpreted as inverted fluvial channels) extending across the crater floor over the bright felsic unit<sup>24</sup>. Some portions of the felsic unit show evidence of minor alteration with absorptions at  $\sim 1.9$  and  $2.4\ \mu\text{m}$  (Fig. 1b, teal), consistent with hydrated sulphate salts or certain zeolites<sup>15</sup>, whereas other portions seem relatively unaltered (Fig. 1b, gold). The felsic outcrops appear deeply eroded, light-toned and smooth, with varying degrees of polygonal fracturing<sup>24</sup>. The polygons exhibit rounded edges and are typically tens of metres in diameter (Fig. 3a,b), allowing CRISM to resolve the felsic spectral character of sand-free outcrop.

Felsic exposures in Noachis Terra are found across an area of at least  $\sim 150,000\ \text{km}^2$ . Some of these outcrops (for example, arrow 4 in Fig. 2) correspond to a so-called red unit identified

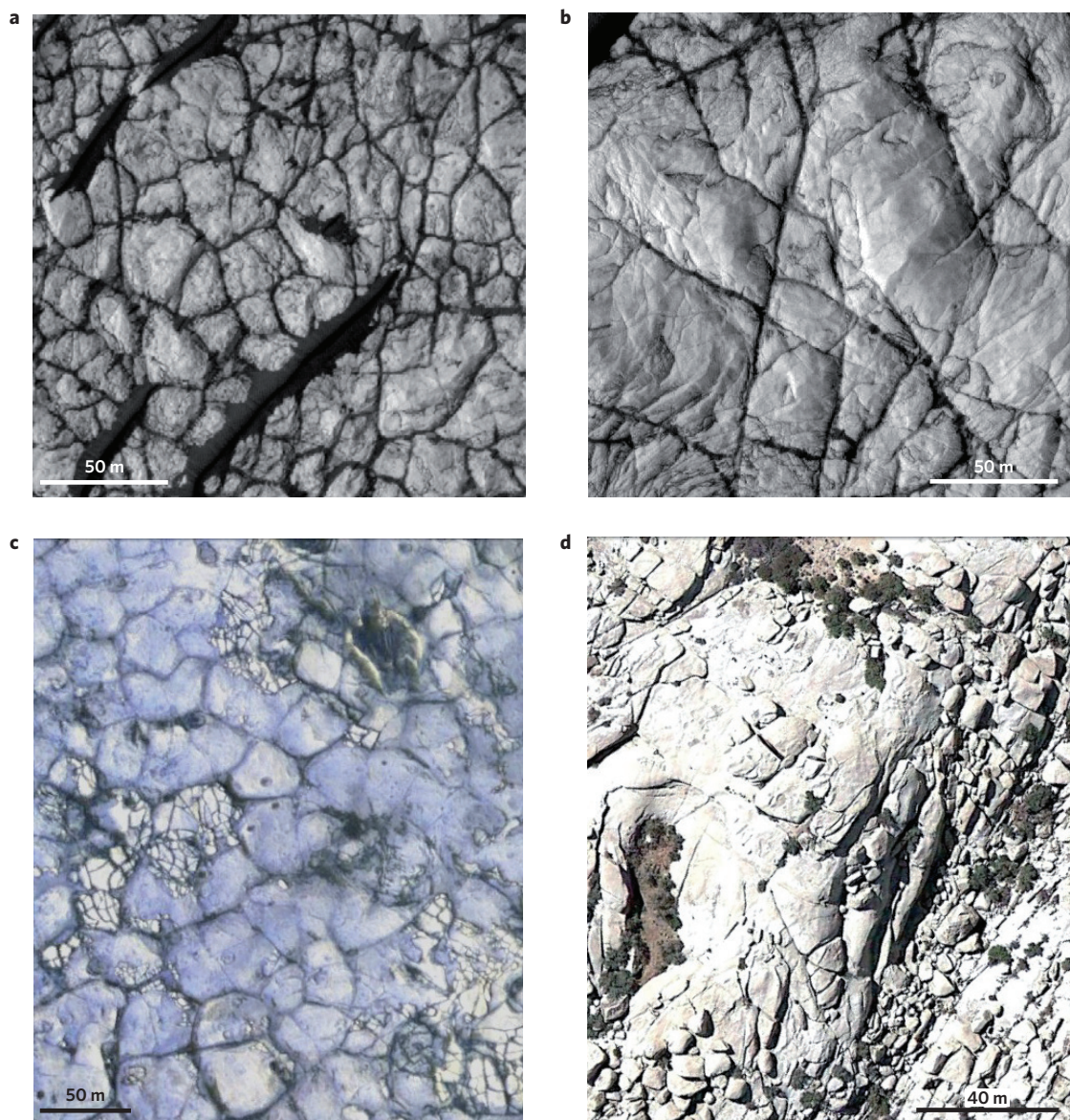


**Figure 3 | Polygonal fracture patterns in felsic rocks on Mars and Earth. a, b**, Two samples of a felsic Noachis Terra crater floor (21.56° S, 41.10° E), from HiRISE ESP\_013504\_1580. **c**, The Nili Patera caldera floor (8.86° N, 67.28° E), from HiRISE PSP\_005684\_1890. **d**, Google Earth image of weathering cracks developed on granite in the arid environment of Joshua Tree National Park (34.032° N, 116.142° W).

in decorrelation-stretched images from the Thermal Emission Imaging System (THEMIS) on Mars Odyssey<sup>19</sup>. This high thermal inertia unit was unresolvable by hyperspectral instruments before CRISM, but THEMIS data suggested a mafic-poor, high-silica and/or sulphate-rich composition relative to other highlands materials<sup>19</sup>. CRISM spectra demonstrate that these are feldspar-rich materials with very low mafic abundances, variably altered to hydrated phases (for example, sulphates).

A third occurrence of felsic rocks, with morphology similar to the Noachis crater floors (Fig. 3c), is found in the Nili Patera caldera (Fig. 4). Felsic rocks are exposed at the lowest elevations within the caldera, where one of the highest thermal inertias measured on Mars implies a clean bedrock exposure<sup>25</sup>. Small remnant mounds scattered across this felsic bedrock suggest it was previously buried beneath at least several metres of eroded material. The central portion of each felsic exposure appears texturally smooth and exhibits the strongest feldspar absorptions (Fig. 1b, orange), whereas peripheral felsic rocks are more chaotically fractured

and display spectral evidence of minor H<sub>2</sub>O (Fig. 1b, dark blue), consistent with physical and chemical weathering.

These felsic rocks lie only ~2 km from the Nili Patera dacitic flow<sup>17</sup>. The association of dacites with more silicic rocks is common on Earth and can be produced by fractional crystallization or partial melting of dacite. To test an analogous origin for the felsic rocks in Nili Patera, we carried out crystallization calculations based on thermodynamic phase equilibria, using several dacitic and intrusive equivalents from Earth and a Mars Pathfinder andesite for our starting compositions. Each rock was comparable in mineralogy to the Nili Patera dacite<sup>17</sup> after renormalization to include only its primary phases (see Supplementary Information). The results were compared with observational constraints from Nili Patera and crystallization calculations for an example tonalite (low-K, intermediate magma) and leucogranite (Supplementary Fig. 2). The extracted melts were more silica-rich than their parent magmas, matching the low pyroxene abundances required by our CRISM observations. This model predicts ~25% quartz or high-Si glass

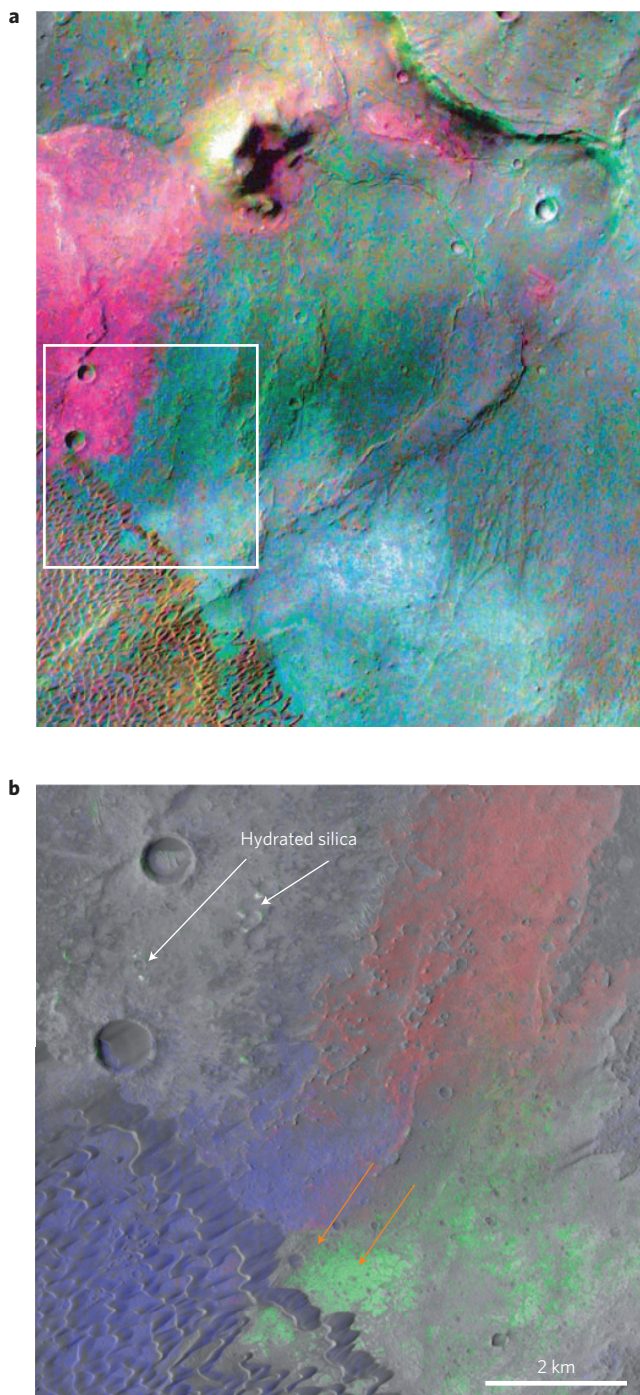


**Figure 4 | Igneous diversity in Nili Patera. a.** Decorrelation-stretched THEMIS infrared bands 9, 7, 5 displayed in red, green, blue (dacite appears magenta), overlain on a THEMIS visible image; reproduced from ref. 17. The white box outlines the area shown in **b. b.** CRISM FRT000082EE spectral parameter maps superimposed on CTX image P04\_002427\_1888. OLINDEX2, confirmed to be mapping olivine, is shown in red; the drop-off from 1.1 to 1.28  $\mu\text{m}$ , mapping felsic rocks, is green; and HCPINDEX, mapping pyroxene, is blue. The orange arrows point to the source areas for the orange (lower right arrow) and dark blue spectra in Fig. 1b.

in the felsic materials, which our observations allow, but we cannot rule out the alternative that these materials in Nili Patera are instead anorthosite.

In contrast with the present paradigm of minimal martian magma evolution<sup>2</sup>, the range of silicic rocks observed in Nili Patera

is consistent with the compositional diversity observed on Earth at sites of prolonged magmatic activity<sup>26</sup>. The Nili Patera dacite has an age of  $\sim 3.0\text{--}3.6$  Gyr based on crater counts<sup>27</sup>, probably postdating the main Early Hesperian phase of Syrtis Major's formation<sup>28</sup>. The felsic rocks seem to underlie basaltic materials with an estimated age of  $2.0 \pm 0.3$  Gyr (ref. 27). These observations imply an Early Amazonian age (between  $\sim 3$  and 2 Gyr) for the felsic rocks if they formed at the surface, or they may be younger if they formed intrusively beneath the basalts.

Some of the felsic outcrops in Noachis Terra (for example, arrow 5 in Fig. 2) have been catalogued among a global population of crater floor bedrock materials attributed to inflationary volcanism following impact-generated fractures in basement rock<sup>20</sup>. If such processes formed felsic rocks, then these rocks probably derived from a relatively high-silica reservoir at depth. Recent CRISM observations of feldspar-rich materials in widely scattered ancient exhumed outcrops<sup>18</sup> may be consistent with such a reservoir. Alternatively, feldspar-rich crater floors could have been emplaced through partial melting of basaltic crust and slow cooling with crystal density separation, processes thought to explain anorthositic plutons on Earth<sup>1</sup>. Some felsic outcrops might also be sedimentary in origin, derived from explosive volcanism or from erosion and transport of igneous materials.

Materials associated with fluvial systems and/or phyllosilicates (as in Xanthe and Noachis Terrae) could have undergone limited feldspar enrichment through selective alteration of more mafic primary lithologies. Feldspars typically weather orders of magnitude more slowly than olivine and—for low-Ca feldspars or certain pH values—factors of  $>2$  more slowly than pyroxene or glass<sup>29,30</sup>. On a world with minimal primary quartz, perhaps fluvially transported sediments became enriched in feldspars (instead of quartz as on Earth), although such processes seem unlikely to yield sediments with  $<5\%$  mafics from basaltic source rocks.

Regardless of how felsic rocks formed, their alteration would have produced more Al/Si-rich secondary phases than would the alteration of basalts. In all locations discussed above, felsic rocks occur near Al-smectites, kaolinite and/or hydrated silica. Numerous locations across Mars exhibit a clay mineral stratigraphy of such Al/Si-rich phases overlying Fe/Mg-rich phyllosilicates, which has been interpreted as evidence for intensive weathering of basalt or of pre-existing Fe/Mg-smectites<sup>15</sup>. Although leaching of cations (Ca, Na) is required to form kaolinite or silica even from felsic precursors, Al-smectites on Mars may more plausibly form from such precursors than from the more mafic-rich primary compositions previously assumed.

Received 30 June 2013; accepted 4 October 2013;  
published online 17 November 2013

## References

1. Winter, J. D. *Principles of Igneous and Metamorphic Petrology* (Prentice Hall, 2010).
2. McSween, H. Y. Jr, Taylor, G. J. & Wyatt, M. B. Elemental composition of the Martian crust. *Science* **324**, 736–739 (2009).
3. Carr, M. H. & Head, J. W. III Geologic history of Mars. *Earth Planet. Sci. Lett.* **294**, 185–203 (2010).
4. Ohtake, M. *et al.* The global distribution of pure anorthosite on the Moon. *Nature* **461**, 236–240 (2009).
5. Cheek, L. C., Donaldson Hanna, K. L., Pieters, C. M., Head, J. W. & Whitten, J. L. The distribution and purity of anorthosite across the Orientale basin: New perspectives from Moon Mineralogy Mapper data. *J. Geophys. Res.* **118**, 1805–1820 (2013).
6. Meslin, P.-Y. *et al.* Soil diversity and hydration as observed by ChemCam at Gale crater, Mars. *Science* **341**, 1238670 (2013).
7. Elkins-Tanton, L. T. Magma oceans in the inner solar system. *Annu. Rev. Earth Planet. Sci.* **40**, 113–139 (2012).
8. Mustard, J. F. *et al.* The surface of Syrtis Major: Composition of the volcanic substrate and mixing with altered dust and soil. *J. Geophys. Res.* **98**, 3387–3400 (1993).

9. Bandfield, J. L., Hamilton, V. E. & Christensen, P. R. A global view of Martian surface compositions from MGS-TES. *Science* **287**, 1626–1630 (2000).
10. Wyatt, M. B. & McSween, H. Y. Jr. Spectral evidence for weathered basalt as an alternative to andesite in the northern lowlands of Mars. *Nature* **417**, 263–266 (2002).
11. McLennan, S. M. Sedimentary silica on Mars. *Geology* **31**, 315–318 (2003).
12. Horgan, B. & Bell, J. F. III. Widespread weathered glass on the surface of Mars. *Geology* **40**, 391–394 (2012).
13. Foley, C. N., Economou, T. & Clayton, R. N. Final chemical results from the Mars Pathfinder alpha proton X-ray spectrometer. *J. Geophys. Res.* **108**, 8096 (2003).
14. Bandfield, J. L., Hamilton, V. E., Christensen, P. R. & McSween, H. Y. Jr. Identification of quartzofeldspathic materials on Mars. *J. Geophys. Res.* **109**, E10009 (2004).
15. Ehlmann, B. L. *et al.* Identification of hydrated silicate minerals on Mars using MRO-CRISM: Geologic context near Nili Fossae and implications for aqueous alteration. *J. Geophys. Res.* **114**, E00D08 (2009).
16. Smith, M. R. & Bandfield, J. L. Geology of quartz and hydrated silica-bearing deposits near Antoniadi crater, Mars. *J. Geophys. Res.* **117**, E06007 (2012).
17. Christensen, P. R. *et al.* Evidence for magmatic evolution and diversity on Mars from infrared observations. *Nature* **436**, 504–509 (2005).
18. Carter, J. & Poulet, F. Ancient plutonic processes on Mars inferred from the detection of possible anorthositic terrains. *Nature Geosci.* <http://dx.doi.org/10.1038/ngeo1995> (2013).
19. Rogers, A. D., Aharonson, O. & Bandfield, J. L. Geologic context of *in situ* rocky exposures in Mare Serpentis, Mars: Implications for crust and regolith evolution in the cratered highlands. *Icarus* **200**, 446–462 (2009).
20. Edwards, C. S., Bandfield, J. L., Christensen, P. R. & Fergason, R. L. Global distribution of bedrock exposures on Mars using THEMIS high-resolution thermal inertia. *J. Geophys. Res.* **114**, E11001 (2009).
21. Adams, J. B. & Goullaud, L. H. Plagioclase feldspars: Visible and near infrared diffuse reflectance spectra as applied to remote sensing. *Proc. Lunar Planet. Sci. Conf.* **9**, 2901–2909 (1978).
22. Serventi, G. *et al.* Spectral variability of plagioclase-mafic mixtures (1): Effects of chemistry and modal abundance in reflectance spectra of rocks and mineral mixtures. *Icarus* **226**, 282–298 (2013).
23. Popa, C., Esposito, F. & Colangeli, L. New landing site proposal for Mars Science Laboratory (MSL) in Xanthe Terra. *41st Lunar Planet. Sci. Conf.* abstract 1807 (2010).
24. Irwin, R. P. III., Wray, J. J., Maxwell, T. A., Mest, S. C. & Hansen, S. T. *3rd Int. Conf. on Early Mars* abstract 7066 (Lunar and Planetary Institute, 2012).
25. Christensen, P. R. *et al.* Morphology and composition of the surface of Mars: Mars Odyssey THEMIS results. *Science* **300**, 2056–2061 (2003).
26. Gunnarsson, B., Marsh, B. D. & Taylor, H. P. Jr. Generation of Icelandic rhyolites: Silicic lavas from the Torfajökull central volcano. *J. Volcanol. Geotherm. Res.* **83**, 1–45 (1998).
27. Robbins, S. J., Di Achille, G. & Hynes, B. M. The volcanic history of Mars: High-resolution crater-based studies of the calderas of 20 volcanoes. *Icarus* **211**, 1179–1203 (2011).
28. Hiesinger, H. & Head, J. W. III The Syrtis Major volcanic province, Mars: Synthesis from Mars Global Surveyor data. *J. Geophys. Res.* **109**, E01004 (2004).
29. Hurowitz, J. A. *et al.* *In situ* and experimental evidence for acidic weathering of rocks and soils on Mars. *J. Geophys. Res.* **111**, E02S19 (2009).
30. Hausrath, E. M., Navarre-Sitchler, A. K., Sak, P. B., Steefel, C. I. & Brantley, S. L. Basalt weathering rates on Earth and the duration of liquid water on the plains of Gusev crater, Mars. *Geology* **36**, 67–70 (2008).

### Acknowledgements

Portions of this work were supported by NASA Mars Data Analysis Program grant NNX13AH80G. We thank B. Horgan for a review and H. McSween, J. Mustard, B. Ehlmann, R. Clark and C. Viviano for discussions.

### Author contributions

J.J.W. carried out the spectral analysis, wrote most of the text and assembled the figures, with assistance from S.T.H. Thermodynamic equilibria models and related text were contributed by J.D. G.A.S. carried out laboratory spectral analyses. S.L.M. and F.P.S. produced the CRISM data products. J.R.S., R.P.I. and M.S.G. provided input on the text.

### Additional information

Supplementary information is available in the [online version of the paper](#). Reprints and permissions information is available online at [www.nature.com/reprints](http://www.nature.com/reprints). Correspondence and requests for materials should be addressed to J.J.W.

### Competing financial interests

The authors declare no competing financial interests.